CHEMICAL ENGINEERING TRANSACTIONS
VOL. , 2023
A publication of AIDIC
The Italian Association of Chemical Engineering
Online at www.cetjournal.it
Guest Editors: David Bogle, Flavio Manenti, Piero Salatino

ISBN 979-12-81206-04-5; **ISSN** 2283-9216

Electro-membrane processes for the green hydrogen production

Alessandra Pellegrino, Giovanni Campisi, Federica Proietto, Alessandro Tamburini*, Onofrio Scialdone, Giorgio Micale

Dipartimento di Ingegneria, Università degli Studi di Palermo, viale delle scienze ed. 6, 90128 Palermo, Italy;
*corresponding author: alessandro.tamburini@unipa.it

Since the last century, humanity has been facing challenging scenarios, like global warming, environmental pollution and the dramatic increase in energy demand. In this framework, green hydrogen has been identified as the most promising energy vector to achieve carbon neutrality. With this respect, the idea of the present work is to combine the Reverse Electrodialysis (RED) membrane process with hydrogen production. Experimental RED tests were carried out by feeding the unit with different concentrated solutions to study the process performance. Collected results suggest that this approach is a viable way to produce hydrogen with high faradic efficiencies, up to a maximum of 99 %, highlighting also the technology advantage of producing hydrogen by exploiting the salinity gradient energy, thus leading to a production with Specific Energy Consumption close to zero.

1. Introduction

The recent sharp increase in world population and energy demand can no longer be satisfied by the use of fossil fuels (United Nations Environment Programme, 2022). As highlighted in the most important international meetings such as COP27 and G20 (IEA, 2019), there is the need to change and move towards the third industrial revolution using renewable energy sources as well as through the use of the most promising green energy carrier: hydrogen (IRENA, 2020). Hydrogen is the most abundant and lightest element in the universe, and it has the highest gravimetric energy density of all known substances, i.e., the lower heating value is about 120 MJ kg^{-1} and high heating value is 141 MJ kg^{-1} (about three times higher than the diesel or gasoline today used). The overall goal would be to store energy in the form of hydrogen for its great properties. Today hydrogen can be produced in several ways, but the future is the green hydrogen production from renewable sources, with zero greenhouse gas (GHG) emissions.
To this aim, the idea of the present work is to produce green hydrogen using membrane technologies, with in situ consumption of all the energy produced by Reverse Electrodialysis (RED), a pollution-free and zero-emission technology. In addition, in this work, it was also considered the idea of using this system not only for the hydrogen production, but also for the desalinated water production, by consuming energy from a power supply with the Electrodialysis (ED) process.
ED/RED is a membrane technology that consists of repetitive units called cell pairs. The repetitive units include anionic (AEM) and cationic (CEM) ion exchange membranes between which net spacers are interposed to create the compartments hosting the saline solutions: the high concentrated salt solution (HC) and the low concentrated salt solution (LC) (Campisi et al., 2023).
Focusing on ED, as shown in Figure 1a, a salty solution enters the system, and a power supply is inserted in the external electrical circuit. Migrative ionic fluxes through the selective membranes occurred in the system, allowing the desalination of the inlet flow at the expense of the adjacent channels where the concentration increases. In this case, the energy provided by the power supply is converted into a salinity gradient of the two outflows (Gurreri et al., 2022).
In Figure 1b, RED technology makes a controlled mixing of two inlet streams with a concentration gradient between them, in order to produce energy. In particular, once the external load is connected to electrical circuit,

the spontaneous diffusive ionic fluxes generated inside the system are transformed into an electronic flux by the reactions that take place at the electrodes. Here, the salinity gradient energy is converted to electric energy.

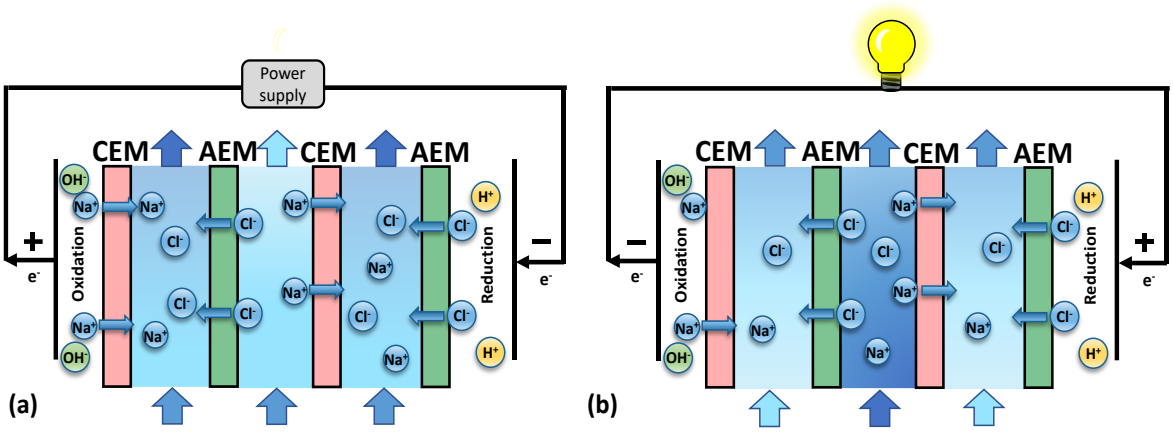

Figure 1. Schematic representation of the two different operation modes of the system: (a) Electrodialysis (ED); (b) Reverse Electrodialysis (RED).

RED has many applications, but the newest ones couple it with hydrogen production. Among the first, Hatzell et al. (2014) developed a new method to treat the acid waste stream with ammonium bicarbonate (AmB) RED, producing hydrogen by consuming the acid to be disposed of. Similarly, using AmB solutions, Raka et al. (2020) conducted thermally driven H_2 production using RED. Chen et al. (2017) evaluated experimental hydrogen production with RED at different NaCl salt concentrations. They obtained a maximum hydrogen productivity of 0.55 mL cm^{-2} h^{-1} (0.25 mol m^{-2} h^{-1}) with faradic efficiency of 84 % – 96 % and a current density of 19.7 A m^{-2}.
On the other hand, Alshebli et al. (2023) was the first who proposed coupling desalination of salt currents (ED) with hydrogen production, using desalination solutions of sodium sulphate (Na_2SO_4).
With this respect, the present work focuses on continuous short-circuit RED tests to maximize hydrogen production with different high concentrated saline solutions. In addition, for the first time, experimental polarization curves are collected both for RED and for ED modes. The experimental feasibility of the desalination process in ED mode is tested using NaCl solutions for the simultaneous production of water and hydrogen.

2. Materials and methods

Two different kind of experimental tests were carried out in the present work: (i) ED/RED polarization curves and (ii) continuous short-circuit RED tests. Continuous short-circuit RED tests were performed by letting the concentration of the concentrated solution to vary while keeping constant the concentration of the diluted one. To ensure test reproducibility, each test was carried out at least twice under the same conditions.

2.1 Stack design and solutions

A co-current flow lab-scale RED unit with an active area of 10 x 10 cm^2 equipped with 20 cell pairs was used for both polarization curves and continuous short-circuit RED tests. The system was assembled with the commercial ion-exchange membranes Fujifilm Type 10 CEM and AEM (Tilburg, The Netherlands), with 300 µm thick woven spacers (Redstack, Sneek, The Netherlands). Platinum wires were inserted inside the last two salt compartments (end-membranes side) to measure the voltage over the stack without the contribution of the electrode compartments. The latter was calculated as the difference between the total voltage of the system minus the one measured with the platinum wires.
The electrodes compartments consist of: (i) Ti mesh grid substrate with Pt/Ir ox. (MMO – Mixed Metal Oxide) electrodes used as cathode and anode chosen on the basis of kinetics studies (Quaino et al., 2014); (ii) catholyte and anolyte, aqueous solutions of HCl 0.5 M and NaOH 0.5 M respectively, solutions chosen for thermodynamic reasons because they allow the reactions (1) and (2); (iii) the two end-membranes, AEM Fujifilm Type 10 (Tilburg, The Netherlands) for the cathode and a Nafion CEM membrane for the anode; (iv) nitrogen was insufflated as stripping gas into the anolyte and the catholyte. The gas outflow from the cathode and the anode compartments was measured in continuous using two Ki-Key Instruments LPM AIR 0.004-0.5 flow meters.

Hydrogen Evolution Reaction (HER) in acid medium:

$$2H^+ + 2e^- \leftrightarrow H_2 \qquad E^0 = 0.0\ V \tag{1}$$

Oxygen Evolution Reaction (OER) in alkaline medium:

$$4OH^- \leftrightarrow O_2 + 2H_2O + 4e^- \qquad E^0 = +0.4\,V \tag{2}$$

The catholyte was prepared by diluting HCl (37 % Merck), while the anolyte was prepared from NaOH pellets (98 –100 % Honeywell Fluka). NaCl (99.7 % ChemSolute) was used to prepare each salt solution.
Two Leadfluid YT15 peristaltic pumps (BT601S, Lead Fluid Technology, CO LTD, China) were used to recirculate the anolyte (volume of 150 ml) and the catholyte (volume of 200 ml) with a flow rate of 525 ml min^{-1}. Two Cole-Parmer Masterflex I/P (77601-00, Illinois, USA) were used to pump the high and low concentrated solutions with a 180 ml min^{-1} flow rate. The two salty solutions were placed in open loop, in order to obtain the same concentrations at the stack inlet and, thus, the same electromotive force during the tests.
The concentration of the salty solutions was measured through ion chromatography (Ion Chromatography Metrohm 882 Compact IC plus), in addition, the conductivity and the pH were monitored using a WTW conductivity and pH meter (WTW™ ProfiLine™ pH/Cond 3320 Universal Multi-parameter Portable).
As far as the electrical circuit is concerned, two Fluke 175 multimeters were used to measure the external stack voltage and the platinum wires voltage, and a Fluke 8808A 5-1/2 Digit Multimeter was used to monitor the current.

2.2 Polarization curves

A power supply (EA PS2042-10B, Elektro-Automatik GmbH & Co.KG) was used for the ED polarization curve measurements. Conversely, a RS PRO Programmable DC Electronic Load RS-KEL103 mimicking an external load was used for the RED polarization curve. Both ED and RED polarization curves were performed in potentiostatic mode. These tests were performed using a low concentrated solution of 1 g L^{-1} NaCl, representing a typical river water concentration, and a high concentrated solution of 35 g L^{-1} mimicking seawater concentration level.
In these tests the power density (PD) was calculated as the product between the voltage (U) and current (I) normalized for the total membrane area, as shown by equation (3):

$$PD = \frac{I\,U}{2\,S_{membr}N_{cp}} = \left[\frac{W}{m^2}\right] \tag{3}$$

where S_{membr} is the membrane surface and N_{cp} is the number of cell pair.

2.3 Continuous short-circuit RED tests

The continuous RED tests were performed in three different scenarios having the same low concentrated solution (1 g L^{-1} NaCl) and different high concentrated solutions, to replicate the driving force resulting from the difference in concentration between river water and: (i) sea water, 35 g L^{-1} NaCl; (ii) Reverse osmosis brine, 70 g L^{-1} NaCl; (iii) post-treatment high concentrated brine, 300 g L^{-1} NaCl. All tests were carried out in short-circuit conditions, so that all the energy produced by the RED was fully consumed inside the system and converted into hydrogen and oxygen production. In all tests, gas samples were taken using a gas-tight syringe (Hamilton Company Gastight 1725 TLL, Grisons, Switzerland) from the anolyte and catholyte gas-tanks and analyzed by gas chromatography. The gas chromatograph used is Agilent 7890B GC provided with a Supelco Carboxen-1000 (60/80) column and a thermal conductivity detector (TCD). Helium of purity 99.999 % supplied by Air Liquide with constant pressure at 1 bar was employed as the carrier gas. The temperature program for the column included an isotherm at 35 °C for 5 minutes followed by a ramp of 20 °C min^{-1} up to 225 °C and an isotherm phase for 40 minutes; the thermal conductivity detector temperature was 230 °C. In addition, samples of anolyte and catholyte solutions were collected for analysis by acid-base titration and spectrophotometry Uv-Vis. These Uv-Vis spectrophotometry tests were conducted using Agilent cary 60 UV spectrophotometer to detect any additional product.
For all continuous tests, key performance indicators were calculated, such as Faradic Efficiency (FE) and Productivity (P). The Faradic Efficiency is the ratio between the charge used to obtain the product and the total charge circulating in the system, calculated as the product (4):

$$\text{Faradic Efficiency (FE)} = \frac{z\,F\,mol_{prod}}{I\,t}100 = [\%] \tag{4}$$

where z is the number of electrons involved in the reaction, F is the Faraday constant and t is the time considered.
The productivity is defined as the quantity of product (mol_{prod}) per hour divided by electrode surface area (S_{electr}) (5):

$$\text{Productivity} = 3600\ \frac{\text{mol}_{\text{prod}}}{\text{t}\ S_{\text{electr}}} = \left[\frac{\text{mol}}{\text{h m}^2}\right] \quad (5)$$

3. Results and discussions

Firstly, polarisation curves in ED and RED modes were analyzed, then the performance of the continuous short-circuit RED tests was investigated.

3.1 Polarization curves

Figure 2a shows the polarization curves collected. In particular, the graphs plot the polarization curves of the system reporting the external voltage and platinum wires measurements.

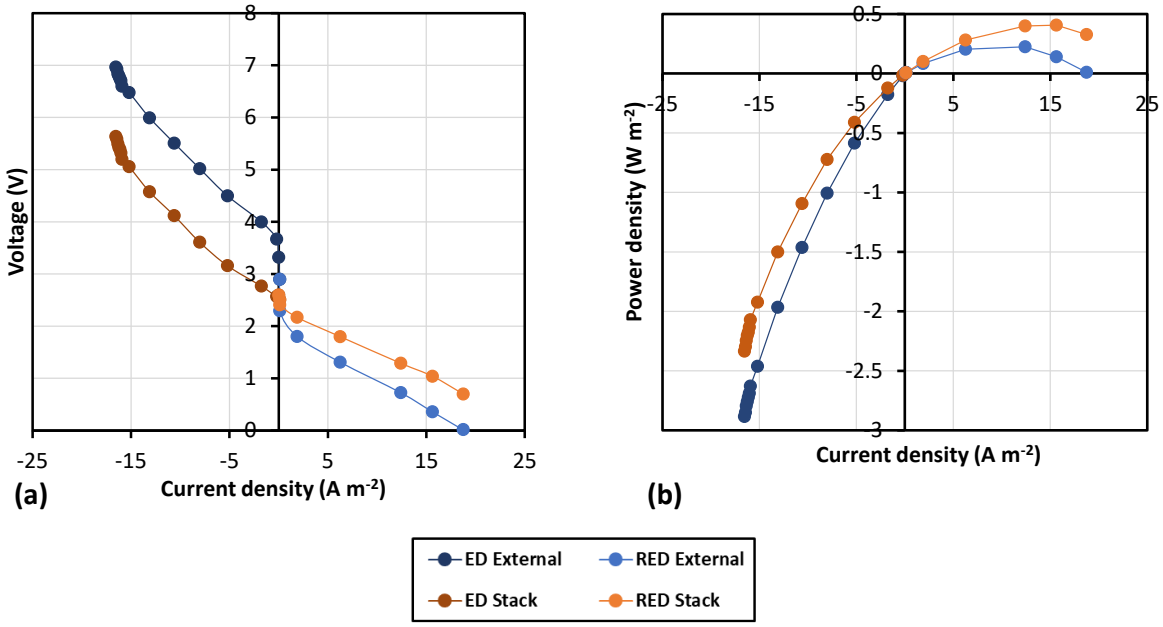

Figure 2. Stack assembled with 20 cell pairs, LC 1 g L^{-1} and HC 35 g L^{-1}, operation of the system in ED and RED modes. (a) External and stack voltage versus current density. (b) External and stack power densities versus current density.

Firstly, it is possible to observe that the external voltage curve in both ED and RED has a very sharp slope at low current densities due to the activation of the electrodes (Saha and Goebel, 2009). At larger current densities a linear trend is found for both ED and RED as expected due to the ohmic control of the process. Trends drastically change for high current densities when the system is operating in ED mode, as shown in Figure 2a. This indicates that mass transport control is taking place in the stack: in other words, system operation is closer to the limiting current density condition. As a matter of fact, the concentration of the dilute channel is so low (i.e. 1 g L^{-1}) that at high currents a further dilution of the channel concentration (as it occurs under ED operation mode) can easily lead to mass transport controlled conditions, notwithstanding the stack length is low. As expected, electrode compartments contribution lead to a lower power produced under RED mode and to a larger power demand under ED mode (Figure 2b). As Figure 2b shows, the maximum power density generated by the RED system with the solutions is approximately of 0.23 W m^{-2}. Figure 2b also shows short-circuit conditions in RED mode are achieved for a current density of about 20 A m^{-2}. Under this condition, the total electromotive force generated is consumed within the RED unit to maximize the production of hydrogen and oxygen. This represents the working point for all continuous tests described below in the next section 3.2.

3.2 Continuous short-circuit RED tests

Continuous tests were carried out in short-circuit RED mode with the same diluted 1 g L^{-1} solution and three different high concentrated solutions: 35 g L^{-1}, 70 g L-1 and 300 g L^{-1}. To analyse the tests, the variation of current over time was observed, and the key performance indicators Faradic Efficiency and productivity of hydrogen were calculated (see Figure 3).

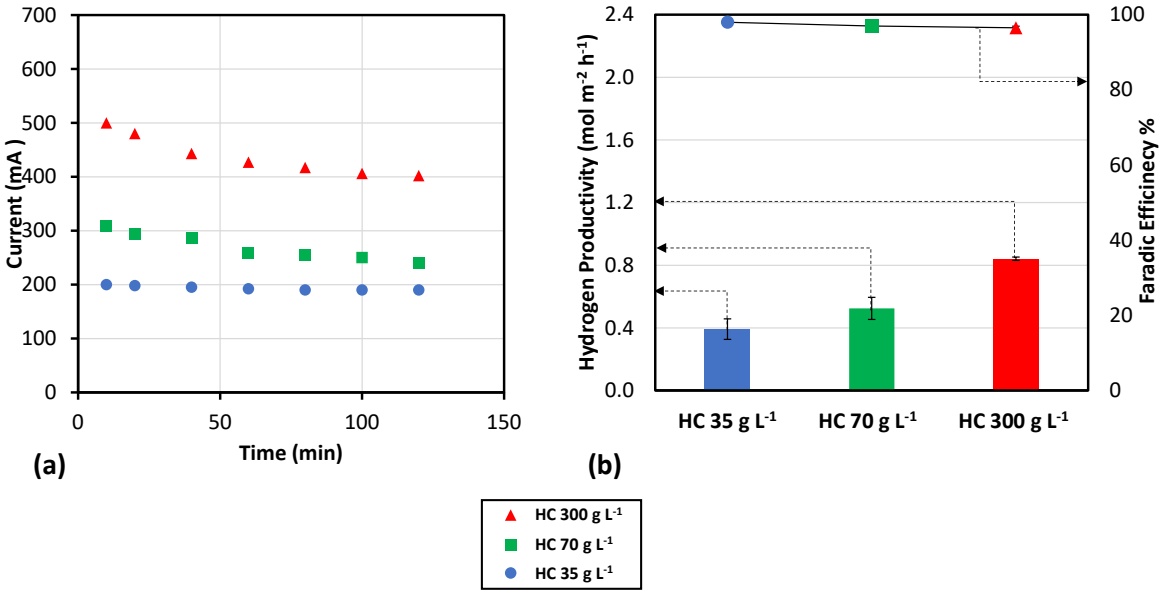

Figure 3. Stack assembled with 20 cell pairs, LC 1 g L^{-1} and three different HC concentrations: 35 g L^{-1}, 70 g L^{-1} and 300 g L^{-1}. (a) Current versus time; (b) Hydrogen productivity and cathodic Faradic Efficiency.

The current versus time trend in the different tests is shown in Figure 3a: (i) the test with HC 35 g L^{-1} started with a short-circuit current around 200 mA, which remained constant for almost the entire duration of the test; (ii) the test with HC 70 g L^{-1} had a short-circuit current starting at 310 mA and decreasing by approximately 20 % at the end of the test; (iii) the test with HC 300 g L^{-1} had a short-circuit current starting at 500 mA and in the same way decreasing by 20 % at the end of the test. These three current trends depended on several factors. First, as the concentration difference between dilute and concentrated solution increases, the electromotive force generated by the system increases, thus leading to higher initial currents. However, there are phenomena that can cause current to decrease over time. The higher the current, the higher the gas evolution and the larger the number of gas bubbles generating at the electrodes. Some bubbles fail to be released by the system causing an increase in the internal resistance with the consequent reduction of the current over time. Another phenomenon that contributes to the current reduction is the time-variation of anolyte and catholyte concentrations.

By acid-base titration and by ion chromatography, the ion concentrations in the solution were determined, so it was possible to understand how they influence the system. Through acid-base titration, it was estimated that the final anolyte and catholyte concentrations of the HC 70 g L^{-1} and HC 300 g L^{-1} tests were 27 % and 45 % respectively lower than the final anolyte and catholyte concentrations of the HC 35 g L^{-1} test. Having lower concentrations means, according to the Nernst equation, that the required thermodynamic potentials for electrode reactions are higher. This result in more energy consumed at the electrodes and in the decrease of the circulating current. In addition, it was observed by ion chromatography that the concentration of chlorides diffused in the electrode compartments increases as HC concentration increases. The concentration of chlorides was found to vary from a minimum of 0.01 M in the HC 35 g L^{-1} test to a maximum of 0.1 M in the HC 300 g L^{-1} test. The presence of chlorides, especially in the anode compartment, could influence the OER (Dresp et al., 2019) and affect the circulating current in the system.

Although in the tests with higher HCs, there is a decrease in terms of current, the performance of the tests has to be analyzed through the key indicators. Figure 3b shows the cathodic faradic efficiency and productivity of hydrogen as the HCs used vary. The cathodic faradic efficiency of hydrogen appears to be between 97 % and 99 % in all tests, so the charge passed in the system is used almost entirely to produce hydrogen at the cathode, and this does not depend on the current values circulating in the system. The productivity of hydrogen is 0.39 mol h^{-1} m^{-2} for the HC 35 g L^{-1} test, 0.53 and 0.84 mol h^{-1} m^{-2} in the HC 70 g L^{-1} test and HC 300 g L^{-1} test, respectively. According to these results, productivity varies linearly with the current.

In this framework, it may be useful to compare the data obtained in this work with other data reported in the literature. For example, Chen et al. (2017) obtained maximum productivities of 0.55 mL h^{-1} cm^{-2} (i.e., 0.25 mol h^{-1} m^{-2}) with faradic efficiency of 84 % – 96 % and a current density of 19.7 A m^{-2}; which are lower than the above-mentioned values obtained in the present work. The great strength of this work is especially that all tests were carried out in short-circuit, with zero external voltage, thus achieving zero Specific Energy Consumption.

The RED produces the energy that is used entirely in the system for hydrogen production, with zero external energy demand.
In addition, it is worth noting that the RED electrolyzer water hydrogen production efficiency is about 65%, a bit lower than state-of-the-art electrolyzers (about 70%), but this value is a valid starting point.

4. Conclusions

Hydrogen is currently considered one of the main clean and green energy carriers of the future. To this aim, the present work is devoted to producing hydrogen in situ using zero-emission Electrodialysis and Reverse Electrodialysis systems. In particular, the polarization curves of the system in the two configurations were obtained. According to these results, very stable trends were observed, except (i) at low current densities in both ED and RED, where there is electrode activation, and (ii) at high current densities in ED, where there is a mass transport limit. In addition, the RED polarization curve produced a maximum power density of 0.23 W m^{-2}. Continuous tests were carried out by fully exploiting the salinity gradient energy produced by RED in the short-circuit condition, in order to maximize the hydrogen produced. The tests were carried out by using the same low concentrated solution and different high concentrated solutions, to observe how hydrogen productivity varies with the salinity gradient. All the tests showed faradic efficiencies close to 100 % while the productivity was found to vary linearly with the current, up to a maximum of 0.84 mol h^{-1} m^{-2}. The technology has the great advantage to operate in short-circuit mode by using all the energy it produces. This makes the unit being self-sustaining thus having a zero Specific Energy Consumption. Clearly, a more detailed study is necessary to comprehensively investigate the electrode contributions, to achieve higher current densities and productivities. Finally, an economic analysis will also carry out to fully assess the economic feasibility of the process.

Nomenclature

E^0– Standard potential, V
F– Faraday constant, C mol^{-1}
FE – Faradic Efficiency, %
HER – Hydrogen Evolution Reaction
I – Current, A
mol_{prod} – quantity of product, mol
N_{cp} – Cell pairs number
OER – Oxygen Evolution Reaction
PD – Power Density, W m^{-2}
S_{membr} – Membrane active surface, m^2
S_{electr} – Electrode active surface, m^2
t – Time, s
U – Voltage, V
z– Number of electrons involved in the reaction

References

Campisi, G., Cosenza, A., Giacalone, F., Randazzo, S., Tamburini, A., Micale, G., 2023. Desalination of oilfield produced waters via reverse electrodialysis: A techno-economical assessment. Desalination 548. doi.org/10.1016/j.desal.2022.116289

Chen, X., Jiang, C., Zhang, Y., Wang, Y., Xu, T., 2017. Storable hydrogen production by Reverse Electro-Electrodialysis (REED). J Memb Sci 544, 397–405. doi.org/10.1016/j.memsci.2017.09.006

Dresp, S., Dionigi, F., Klingenhof, M., Strasser, P., 2019. Direct electrolytic splitting of seawater: Opportunities and challenges. ACS Energy Lett., 933-942. doi.org/10.1021/acsenergylett.9b00220

Gurreri, L., La Cerva, M., Moreno, J., Goossens, B., Trunz, A., Tamburini, A., 2022. Coupling of electromembrane processes with reverse osmosis for seawater desalination: Pilot plant demonstration and testing. Desalination 526. doi.org/10.1016/j.desal.2021.115541

Hatzell, M.C., Zhu, X., Logan, B.E., 2014. Simultaneous hydrogen generation and waste acid neutralization in a reverse electrodialysis system. ACS Sustain Chem Eng 2, 2211–2216. doi.org/10.1021/sc5004133

IEA, 2019. The Future of Hydrogen, IEA, Paris, www.iea.org/reports/the-future-of-hydrogen, License: CC BY 4.0

IRENA, 2020. Green Hydrogen Cost Reduction: Scaling up Electrolysers to meet the 1.5ºC Climate Goal, International Renewable Energy Agency, Abu Dhabi.

Quaino, P., Juarez, F., Santos, E., Schmickler, W., 2014. Volcano plots in hydrogen electrocatalysis-uses and abuses. Beilstein Journal of Nanotechnology 5, 846–854. doi.org/10.3762/bjnano.5.96

Saha, B., Goebel, K., 2009. Modeling Li-ion battery capacity depletion in a particle filtering framework, Annual conference of the Prognostics and Health Management Society.

United Nations Environment Programme, 2022, Emissions Gap Report 2022: The Closing Window — Climate crisis calls for rapid transformation of societies. Nairobi. www.unep.org/emissions-gap-report-2022